Available online at www.sciencedirect.com
ScienceDirect
Pattern Recognition 40 (2007) 3325–3335
PATTERN RECOGNITION
THE JOURNAL OF THE PATTERN RECOGNITION SOCIETY
www.elsevier.com/locate/pr

Evaluation of the effects of Gabor filter parameters on texture classification

Francesco Bianconi[a,*], Antonio Fernández[b]

[a]*Dipartimento Ingegneria Industriale, Università degli Studi di Perugia, Via G. Duranti 67, 06125 Perugia, Italy*
[b]*Departamento de Diseño en Ingeniería, Universidad de Vigo, E.T.S.I.I., Campus Universitario, 36310 Vigo, Spain*

Received 9 February 2006; received in revised form 5 March 2007; accepted 16 April 2007

Abstract

Gabor filtering is a widely adopted technique for texture analysis. The design of a Gabor filter bank is a complex task. In texture classification, in particular, Gabor filters show a strong dependence on a certain number of parameters, the values of which may significantly affect the outcome of the classification procedures. Many different approaches to Gabor filter design, based on mathematical and physiological consideration, are documented in literature. However, the effect of each parameter, as well as the effects of their interaction, remain unclear. The overall aim of this work is to investigate the effects of Gabor filter parameters on texture classification. An extensive experimental campaign has been conducted. The outcomes of the experimental activity show a significant dependence of the percentage of correct classification on the smoothing parameter of the Gabor filters. On the contrary, the correlation between the number of frequencies and orientations used to define a filter bank and the percentage of correct classification appeared to be poor.

Keywords: Gabor filters; Texture classification; Design of experiments

1. Introduction

Texture classification is a topic where scientific interest is currently high. Among the various techniques which have been proposed, Gabor filtering has emerged as one of the leading approaches. The capability of texture discrimination of Gabor functions seems to be related both to their optimal joint resolution in space and frequency, and to their aptitude of modeling the response of cortical cells (*simple cells*) devoted to the processing of visual signals. The link between Gabor functions and the visual system of mammals has been investigated and discussed by various authors. Daugman [1] found that in the cat, the behavior of simple cells could be conveniently modeled with Gabor functions. The experiments performed by Hubel and Wiesel [2] demonstrated that, again in the cat, the simple cells were characterized by a spatial-angular bandwidth of about 30°. Pollen and Ronner [3] suggested that the frequency bandwidth of simple cells is approximately one octave. Other authors found different frequency bandwidths, ranging from 0.5 to 2.5 octaves, clustering around 1.2 and 1.5 [4].

Although Gabor filters are widely adopted, they suffer from certain limitations, mainly because they depend on various parameters that need to be set properly. This problem, sometimes referred to as filter bank design, involves the selection of a suitable number of filters at different orientations and frequencies. In addition, as detailed later, the smoothing parameters may play and important role, and should be chosen carefully. For such reasons the design of a Gabor filter bank, sometimes, resembles to somewhat esoteric, and it is possible to find, in literature, many different approaches. Literature survey, in fact, shows that Gabor filters are implemented in various ways, with different values of filter parameters, resulting in different filter banks. A comparison of the filter banks proposed and discussed in literature is difficult, since the classification procedures are applied to different groups of textures, making the results not comparable. To the best of our knowledge only one work [5] compares the performance of different Gabor filters on image retrieval, taking into account the total number of frequencies and orientation of the filter bank. However, the significance of the parameters is not clarified, nor the effects of the smoothing parameters and of the frequency sampling are taken into account.

The main objective of this paper is a systematic evaluation of the effects of Gabor filter parameters on texture classification.

* Corresponding author. Tel.: +39 755853706; fax: +39 755853703.
E-mail address: bianco@ieee.org (F. Bianconi).

0031-3203/$30.00
doi:10.1016/j.patcog.2007.04.023

In particular we want to investigate the following aspects:

- among the parameters that come into play in Gabor filter design, identify those with significant effects on texture discrimination and
- evaluate the effect of the significant parameters on texture classification.

To pursue these results we adopted an approach based on *design of experiments*. To the best of our knowledge such analysis has not been conducted so far.

The effects of rotation and/or scale variance are beyond the scope of this paper. Further investigation would be necessary to extend the conclusions presented here to textures with varying orientations and/or scales.

2. Theoretical aspects and related research

A two-dimensional Gabor filter consists of a sinusoidal wave modulated by a Gaussian envelope. It performs a localized and oriented frequency analysis of a two-dimensional signal. The formulation in the spatial domain is the following [6]:

$$\psi(x, y) = \frac{F^2}{\pi\gamma\eta} e^{-F^2[(x'/\gamma)^2+(y'/\eta)^2]} e^{i2\pi F x'}, \quad (1)$$

with:

$$x' = x\cos\theta + y\,\mathrm{sen}\,\theta,$$

$$y' = -x\,\mathrm{sen}\,\theta + y\cos\theta, \quad (2)$$

where F is the central frequency of the filter, θ is the angle between the direction of the sinusoidal wave and the x-axis of the spatial domain, γ and η the standard deviations of the Gaussian envelope, respectively, in the direction of the wave and orthogonal to it. These last two parameters (sometimes referred to as the *smoothing* parameters) represent the shape factor of the Gaussian surface: they determine the greater or less selectivity of the filter in the spatial domain. In the above formulation it is assumed that the angle between the wave direction and the axis of the Gaussian envelope is zero.

In the frequency domain the Gabor filter can be written as follows:

$$\Psi(u, v) = e^{-\pi^2/F^2[\gamma^2(u'-F)^2+\eta^2 v'^2]}, \quad (3)$$

with

$$u' = u\cos\theta + v\,\mathrm{sen}\,\theta,$$

$$v' = -u\,\mathrm{sen}\,\theta + v\cos\theta. \quad (4)$$

The design of a filter bank consists in the selection of a proper set of values for the filter parameters: F, θ, η and γ. The possible combinations of the various parameters determine how the filter bank analyzes the spatial and frequency domain.

During the last years various authors proposed and discussed different filter banks for various applications. It is widely accepted that the Gabor filter parameters that most influence texture classification accuracy are: the central frequency of the filter at the highest frequency (F_M), the total number of frequencies (n_F) and the total number of orientations (n_O). It is commonly assumed that the ratio between the central frequency of the filter at frequency (F_n) and that of the filter at the next lower frequency (F_{n-1}) (here referred to as the *frequency ratio* $F_r = F_n/F_{n-1}$) is constant. Sometimes this parameter is referred to as the *frequency progression* [7]. Another common assumption is that the angular spacing among the filters is uniform.

Table 1
Review of some Gabor filter banks proposed in literature

	n_F	n_O	F_M
Turner (1986) [8]	4	4	1/4
Jain and Farrokhnia (1991) [9]	7	4	$\sqrt{2}/4$
Manjunath and Ma (1996) [10]	4	6	0.4
Jain et al. (1997) [11]	5	4	$\sqrt{2}/4$
Kruizinga and Petkov (1999) [12]	3	8	1/5.47
Rubner (1999) [13]	4	6	0.3
Li and Shawe-Taylor (2004) [14]	4–6	4–6	0.4
Clausi and Deng (2005) [15]	4	4	$\sqrt{2}/4$

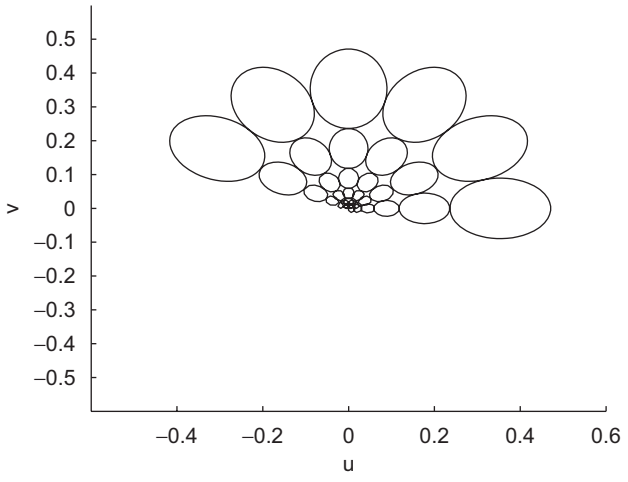

Fig. 1. Filter bank with half-peak magnitude iso-curves touching each other.

Table 1 summarizes some parameter values adopted in literature. The number of frequencies ranges from 3 to 7, the number of orientations from 4 to 8. The central frequency of the filter at the highest frequency is usually chosen to maintain the filter response inside the region delimited by the Nyquist frequency (0.5). The most commonly adopted values are $\sqrt{2}/4$ and 0.4. The frequency values are here expressed in pixels^{-1}.

Most authors adopted the octave interval as frequency ratio [8–11,15], resulting in what it is called *dyadic* decomposition of the frequency domain [16]. Different values, however, have also been adopted, such as in Ref. [12], where the half-octave interval is adopted.

Another common practice is to select the smoothing parameters in order that the half-peak magnitude iso-curves of the filter bank touch each other in the frequency plane (Fig. 1).

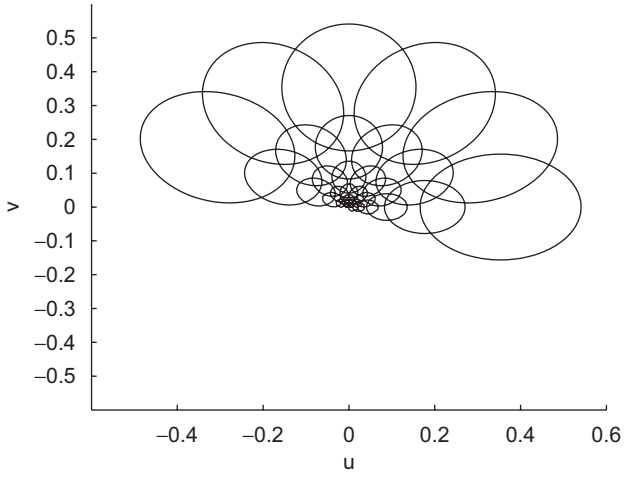

Fig. 2. Filter bank with a certain degree of overlap.

The effect of this design choice is the minimization of the superposition between adjacent filters (as a comparison Fig. 2 shows a filter bank with a certain degree of superposition). It is believed that minimizing the superposition (and hence non-orthogonality) between the various filters of the bank would have beneficial effect on texture discrimination [10]. This assumption, however, is not supported by experimental evidence, since the approach of minimizing superposition has not been compared with others. Moreover it has been shown [17] that orthogonal wavelet transforms suffer from lack of translation invariance, making the content of wavelet sub-bands unstable under translation of the input signal. This may have negative results on texture discrimination.

The smoothing parameters η and γ usually received less attention in literature. Based on physiological outcomes, it is believed that a η/γ ratio of approximately $\frac{2}{3}$ would improve texture discrimination [8]. Nevertheless the data available in literature do not permit any comparison among the effects of different values of the smoothing parameters on texture discrimination.

Literature review suggests that, in general, the selection of a suitable set of parameters for Gabor filtering has been dealt with in various ways, and a comprehensive approach has not come out yet. What remains unclear, in particular, is the effect of the Gabor filter parameters on texture classification.

3. Experimental activity

An experimental campaign has been conducted in order to investigate the effects of Gabor filter parameters on texture classification. Eighty different textures have been used, 40 of them have been taken from the Outex database [18] and 40 from the Brodatz album [19].

The textures have been divided into eight different groups, as shown in Tables 2–4. Following what suggested by other authors [14], aiming at preparing a challenging data set, the textures of each group have been chosen in order to have, in each group, similar and different textures. Each texture has been divided into 16 non-overlapping sub-images of dimension 128×128 pixels, resulting in 160 images for each group.[1]

Table 2
Textures used in the experimental activity (groups 1–3)

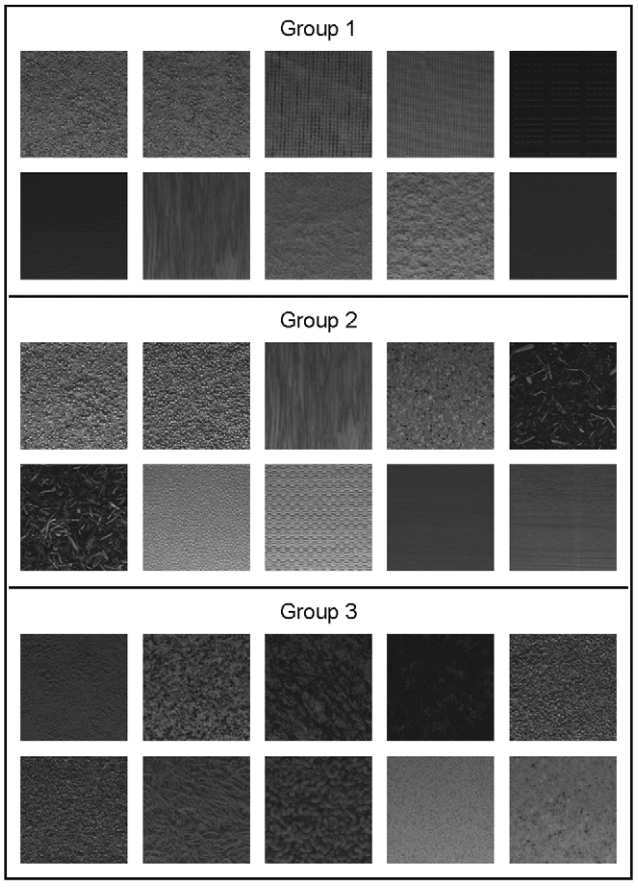

We use different experimental data sets in order to evaluate the significance of the filter parameters on classification accuracy through the *analysis of variance*, which requires the output variable (the success rate) to be computed over different experimental groups. If we had grouped all the textures together, we would have get only a single value of the success rate for each combination of the filter parameters, making it difficult to draw meaningful conclusions from the experiment.

The experimental activity has been focused on the analysis of the effects of Gabor filter parameters on the percentage of textures correctly classified. To accomplish this task a factorial design has been adopted, as described in Section 3.2. The texture classification approach is described here below.

3.1. Texture classification

Texture classification follows a typical procedure, which involves the definition of a feature space, the choice of a

[1] The images used in the experimental activity can be downloaded at the following URL: http://dismac.dii.unipg.it/bianco/download/public/TextureClassification/.

Table 3
Textures used in the experimental activity (groups 4–6)

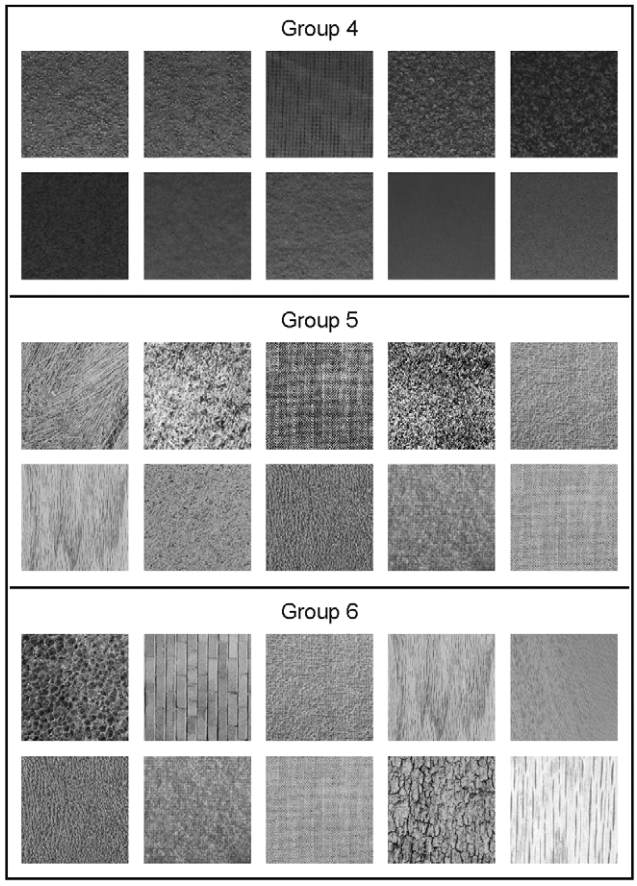

Table 4
Textures used in the experimental activity (groups 7 and 8)

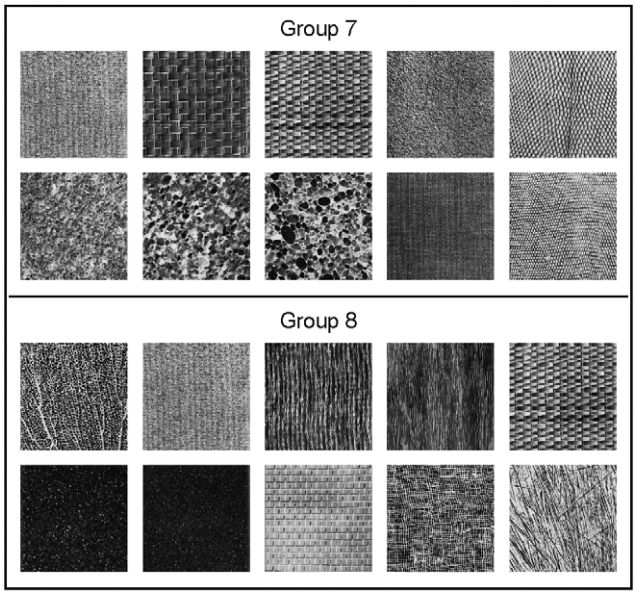

distance measure in the feature space and the adoption of a suitable classification method.

3.1.1. Feature representation

Feature extraction follows an approach commonly adopted in literature [10,14,20,21]. Given an input image $I(w,h)$ of dimensions $W \cdot H$ and a bank of digital Gabor filters $G_{ij}(w,h)$ with $i \in \{1,\ldots,n_F\}$ and $j \in \{1,\ldots,n_O\}$, the Gabor transform of the input image is computed for each filter of the bank as follows:

$$T_{ij}(w,h) = \sum_{a=1}^{W}\sum_{b=1}^{H} I(a,b)\bar{G}_{ij}(w-a,h-b), \tag{5}$$

where $\bar{}$ denotes the complex conjugate.

In order to eliminate the bias related to different illumination [22], we adopted here an implementation of Gabor filters which permits normalization for illumination invariance, as described in Ref. [6].

The mean μ_{ij} and the standard deviation σ_{ij} of the magnitude of each transformed image are used as elements of the feature vector:

$$\mu_{ij} = \frac{1}{WH}\sum_{h=1}^{H}\sum_{w=1}^{W} |T_{ij}(w,h)|, \tag{6}$$

$$\sigma_{ij} = \frac{1}{WH}\sum_{h=1}^{H}\sum_{w=1}^{W} \sqrt{(|T_{ij}(w,h)| - \mu_{ij})^2}. \tag{7}$$

The feature vector $\vec{V}$ is then constructed as follows:

$$\vec{V} = (\mu_{11}, \sigma_{11}, \ldots, \mu_{1n_O}, \sigma_{1n_O}, \mu_{21}, \sigma_{21}, \ldots, \mu_{n_F n_O}, \sigma_{n_F n_O}). \tag{8}$$

3.1.2. Distance measure

Different types of distances to compare color and texture have been proposed and discussed in literature [23]. In a previous work [24] the authors compared the performance of the following distances: L_1, L_2, *Euclidean*, *standardized Euclidean*, *cosine* and *correlation*. The results were suggestive of a better response of the standardized Euclidean with respect to the others. Based on these results we adopted the standardized Euclidean distance to compare textures in the feature space, which is defined as follows:

$$d(\vec{V}_a, \vec{V}_b) = \sum_{i=1}^{p}\sqrt{\left(\frac{V_{ai} - V_{bi}}{\sigma_i}\right)^2}, \tag{9}$$

where σ_i is the standard deviation of the ith dimension over the entire database and p the length of the feature vector, which, in this case, is equal to $2n_F n_O$.

3.1.3. Classification procedure and comparison of classifiers

The classification procedure is based on the k-nn algorithm, with $k = 1$ (nearest neighbor classification). Comparison of classifiers resulting from different filter banks is based on the *split-sample* approach [25]. For each texture group, one-half of the images is used as *training* and the other half as *test*. The percentage of success is computed as the ratio between the number of images of the test group that have been correctly

classified and the total number of images of the test group. The classification is repeated 100 times for each group: each time the images are assigned to the train and test group randomly. The resulting mean percentage of correct classification is computed as the average value over the 100 problems. The way the images are assigned to the test and train group over the 100 problems is the same for all the eight groups of textures.

3.2. Design of experiments

A set of experiments has been designed in order to evaluate the effects of the filters parameters on the percentage of correct classification. In order to draw meaningful conclusions from the results, a statistical design of experiments approach [26] was adopted, based on the use of factorial designs. With factorial designs all the possible combinations of the levels of the factors are investigated. As specified below, five parameters have been considered here as *design factors*, while the *response variable* is represented by the percentage of correct classification.

3.2.1. Design factors

The design of a Gabor filter bank consists, in general, in the selection, for each filter, of the proper values of the following parameters: *central frequency*, *orientation*, η and γ. In this work, as in the majority of the approaches described in literature, we adopted the following assumptions:

- the angular displacement of two adjacent filters is constant (uniform separation in orientation) and
- the frequency ratio of two adjacent filters is constant.

According to these assumptions, a Gabor filter bank is fully determined once the following parameters have been set: the central frequency of the filter at the highest frequency (F_M), the total number of frequencies (n_F), the frequency ratio (F_r), the total number of orientations (n_O) and the values of the smoothing parameters (η and γ).

In order to choose the proper value for the central frequency of the filter at the highest frequency, we adopted two different approaches, resulting in two different groups of experiments: in the first case (*option* 1), in compliance with what suggested by several authors (Table 1), we set the fixed value of $F_M = \sqrt{2}/4$ as the same for all the filter banks; in the second one (*option* 2) the value of F_M is indirectly computed given the value of γ:

$$F_M = \frac{\gamma}{2(\gamma + (\sqrt{\log 2}/\pi))}. \tag{10}$$

This last formula makes the half-peak magnitude iso-curve of the filter at the highest frequency touch the value of $\frac{1}{2}$ (Nyquist frequency), as explained in Appendix C.

Given the value of F_M, the values of n_F, n_O, η and γ have been factorized in a mixed full factorial design as shown in Table 5. Such factorial design results in 162 Gabor filter banks, which have been applied to the eight texture groups, giving 1296 classification tasks (2592 in total, considering the two different approaches adopted to compute F_M). The classification tasks required around 300 h of computation on a laptop equipped with AMD Athlon 1600 processor and 512 Mb RAM.

Table 5
Factorial design

Parameter	Symbol	Levels	Values
Frequency ratio	F_r	2	$\sqrt{2}$, 2
Number of frequencies	n_F	3	4, 5, 6
Number of orientations	n_O	3	4, 6, 8
Eta	η	3	0.5, 1.0, 1.5
Gamma	γ	3	0.5, 1.0, 1.5

Table 6
Effect of the parameters (*option* 1).

Parameter	Symbol	*P*-value	Significant
Frequency ratio	F_r	<0.001	Yes
Number of frequencies	n_F	0.252	No
Number of orientations	n_O	0.281	No
Eta	η	<0.001	Yes
Gamma	γ	<0.001	Yes

4. Evaluation of the results

4.1. Option 1

Table 6 summarizes the analysis of variance over the response, in terms of percentage of correct classification, over the eight groups of textures. The parameters which have significant effects can be identified through the *P-value* [26]. The results suggest that the significant parameters are: *frequency ratio*, η and γ.

4.1.1. Main effects

Fig. 3 shows the main effects of the parameters on the percentage of correct classification. It appears that the effects of the number of frequencies and the number of orientations on the percentage of correct classification are negligible. This in accordance with the outcomes of the analysis of variance, which states these two parameters are not significant.

The main effect of the frequency ratio shows a significantly better performance, on average, of the level 1 ($F_r = \sqrt{2}$, corresponding to half-octave frequency spacing) in comparison with the level 2 (octave frequency spacing).

The main effects of η and γ, show that the percentage of correct classification decreases as the level of the two parameters increases. The effect of γ is stronger. In other words this means that, in terms of main effects, the percentage of classification decreases as the values of η and γ increase. Smaller half-peak magnitude iso-curves of the filters (higher selectivity in the frequency domain) results in a reduction of the percentage of correct classification.

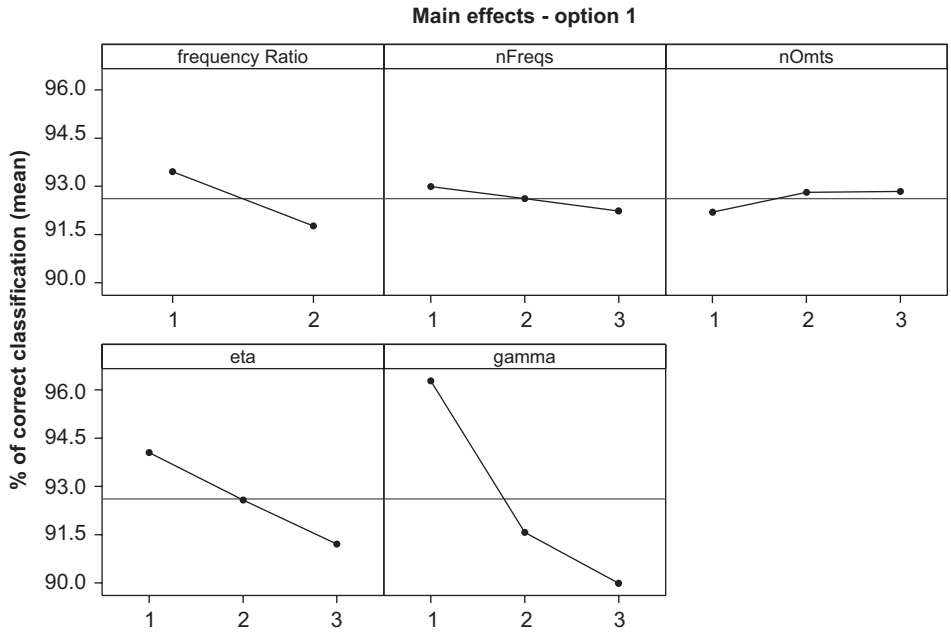

Fig. 3. Main effects plot (*option* 1).

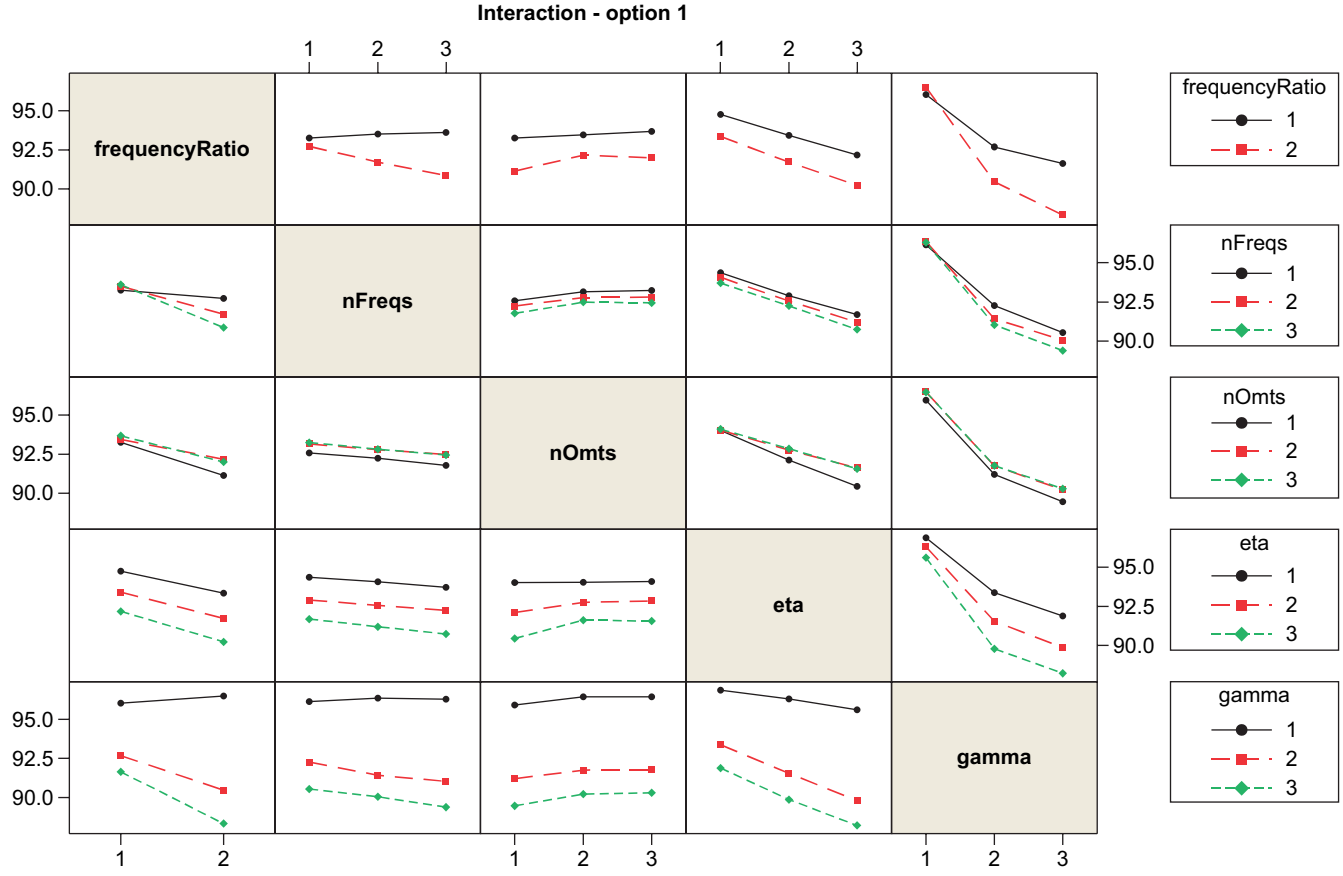

Fig. 4. Interaction plot (*option* 1).

4.1.2. Interaction

Fig. 4 shows the interaction plot for first order interaction. The results, in general, are not suggestive of strong interaction effects. A certain degree of interaction can be observed between γ and F_r (when γ is at level 1, as F_r increases the response increases; when γ is at level 2 or 3, as F_r increases the response

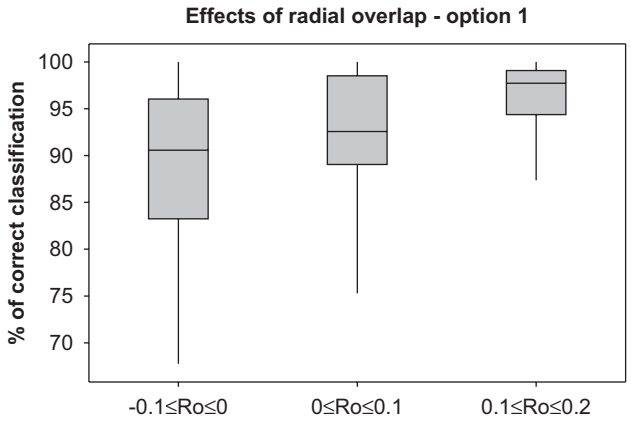

Fig. 5. Effects of radial overlap (*option* 1).

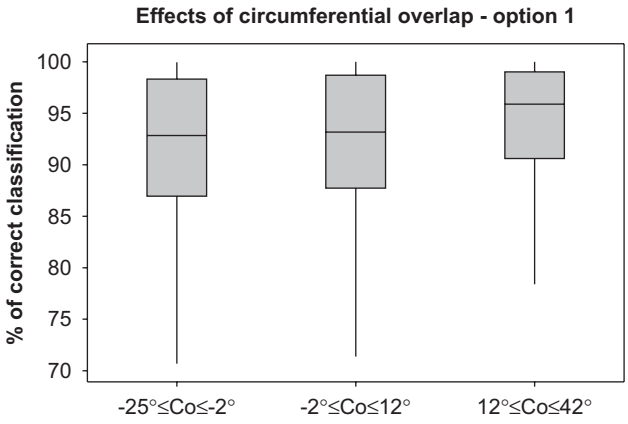

Fig. 6. Effects of circumferential overlap (*option* 1).

decreases). A weak degree of interaction can be also observed between F_r and n_F (when F_r is at level 1, as n_F increases the response increases; when F_r is at level 2, as n_F increases the response decreases).

4.1.3. Effects of filters overlap

It is known that, being Gabor wavelets a non-orthogonal basis, there is redundant information in the transformed images. A common approach in designing Gabor filter banks is to reduce this redundancy by ensuring that the half-peak magnitude iso-curves of the filters responses touch each other [9,10,27,28]. However, it remains unclear whether this approach yields the highest success rate in texture classification, since, to the best of our knowledge, comparative studies have not been published yet. It is also true that different frequency domain coverages, with a certain degree of overlapping among the filters, have been adopted by other authors [12], with good results.

In the experimental activity carried out in this work we tried to investigate the correlation between filters overlap and the percentage of correct classification. In order to do this we introduced two parameters to quantify the overlap of the filters in frequency domain both in the radial and in the circumferential direction: *radial overlap* (R_O) and *circumferential overlap* (C_O). The definitions are given in Appendices A and B.

Fig. 5 shows the effects of radial overlap on percentage of correct classification. The filter banks have been divided into three groups, according to radial superposition, such as that the number of filter banks is the same for each group. The results show, that, on average, the group with the highest radial superposition value performs better both in terms of average correct classification rate, and in terms of less variance.

The effects of circumferential superposition are shown in Fig. 6. As for radial superposition the filter banks have been divided with the criterion of same number for each group. In this case the results do not suggest a strong correlation.

4.2. Option 2

The analysis of variance and of the main and interaction effects are suggestive of conclusions similar to those summarized for option 1. Table 7 reports the analysis of variance over the response, in terms of percentage of correct classification, over the six groups of textures. As for option 1, the results show that the significant parameters are: *frequency ratio*, η and γ.

Table 7
Effect of the parameters (*option* 2)

Parameter	Symbol	*P*-value	Significant
Frequency ratio	F_r	<0.001	Yes
Number of frequencies	n_F	0.058	No
Number of orientations	n_O	0.101	No
Eta	η	<0.001	Yes
Gamma	γ	<0.001	Yes

The main effect plot (Fig. 7) and the interaction plot (Fig. 8) show the same trends of the corresponding graphs obtained for option 1.

The effects of radial (Fig. 9) and circumferential (Fig. 10) overlap appears to be the same as in option 1.

4.3. Comparison between options 1 and 2

Table 8 summarizes the results obtained using the two different design option for Gabor filtering, options 1 and 2. The results show that the two options have comparable results in terms of maximum percentage of correct classification, but option 2 provides a better response in terms of higher overall mean percentage of success and less variance. The difference in the response between the two options was statistically significant ($P < 0.001$).

5. Discussion

The outcomes of the experimental activity are suggestive of interesting considerations, which are summarized here below.

5.1. Significant parameters

From a statistical standpoint, the significant parameters are: the *frequency ratio* F_r and the *smoothing parameters* η and γ.

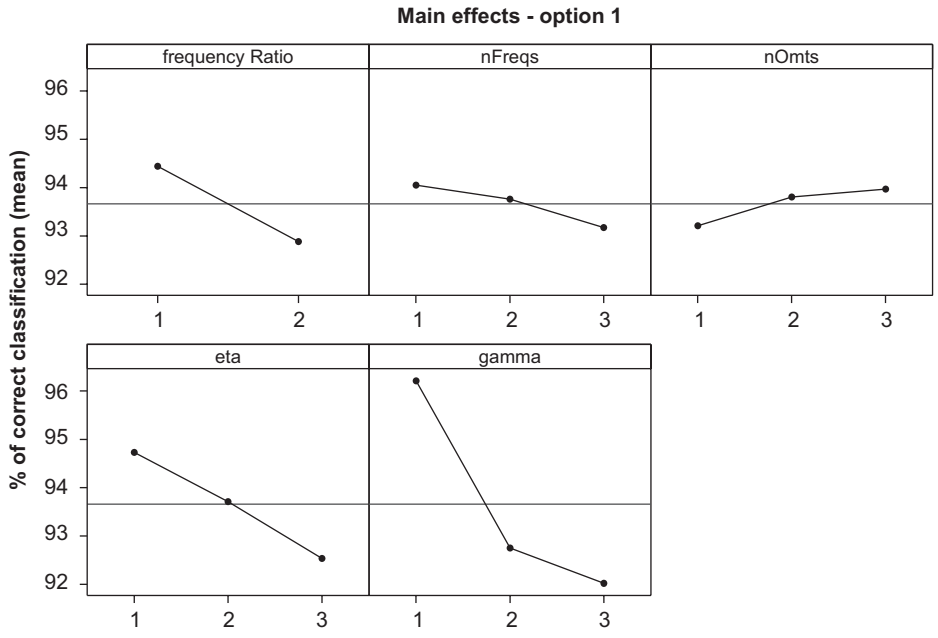

Fig. 7. Main effects plot (*option* 2).

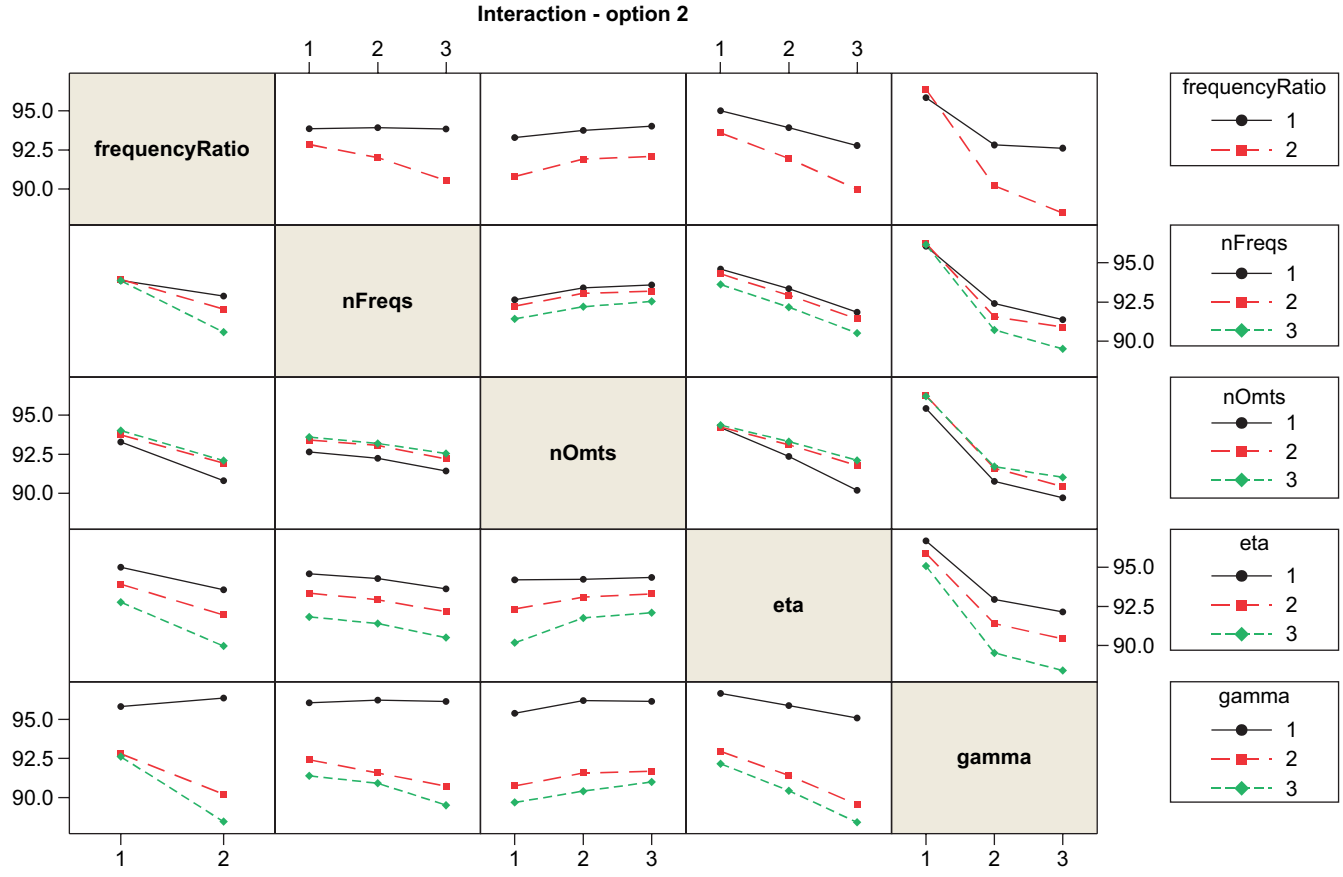

Fig. 8. Interaction plot (*option* 2).

The number of orientations did not show significant effects on the percentage of correct classification. Very little improvement can be appreciated as the number of orientations raises from 4 to 8. This suggests that increasing the number of orientations would only produce a considerable waste of computational time, without tangible beneficial effects.

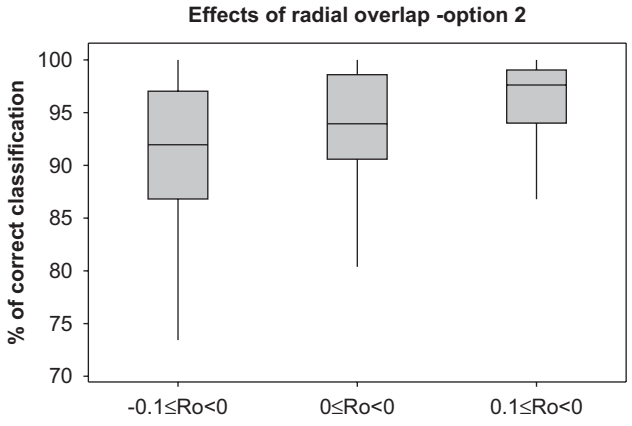

Fig. 9. Effects of radial overlapping (*option* 2).

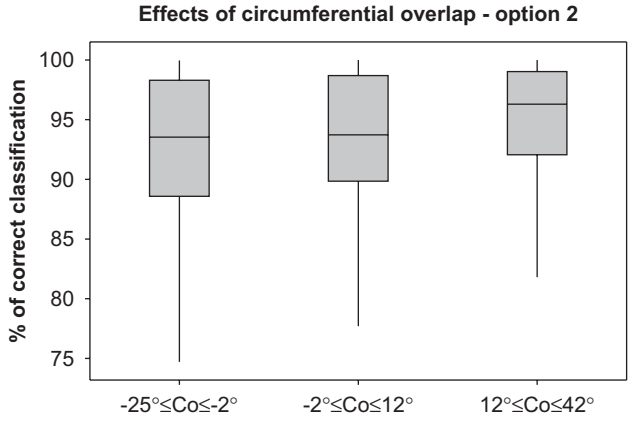

Fig. 10. Effects of circumferential overlapping (*option 2*).

Table 8
Comparison between *options* 1 and 2

	Option 1				Option 2			
	Max	Min	μ	σ	Max	Min	μ	σ
Group 1	99.85	87.75	94.71	3.54	99.82	89.58	95.17	3.16
Group 2	91.24	76.2	84.01	3.84	91.03	74.71	84.33	3.82
Group 3	98.91	73.74	91.91	5.36	98.9	78.32	93.23	4.33
Group 4	98.12	67.76	85.06	9.13	97.32	73.44	90	4.7
Group 5	99.18	81.36	92.11	4.89	99.18	82.45	92.85	4.42
Group 6	99.88	94.7	98.58	1.12	99.86	95.11	98.7	0.88
Group 7	98.86	88.26	94.74	2.29	99.27	90.4	95.2	2.15
Group 8	100	98.61	99.78	0.31	100	98	99.78	0.34
Overall	100	67.76	92.61	7.04	100	73.44	93.66	5.69

The number of frequencies has no significant effect. Substantial variations cannot be appreciated when the number of orientations raises from 4 to 6.

5.2. Effects of F_r, η and γ

The results show that the half-octave frequency sampling, on average, performs better that the octave sampling.

Regarding the effects of η and γ, it appears that the best classification performance is obtained when the two parameters are at their lowest level. This means that low selectivity in the frequency domain (or, alternatively, higher selectivity in the space domain) has beneficial effects on texture classification.

5.3. Correlation with radial and circumferential superposition

Interesting results came out from the analysis of the correlation between filter superposition and percentage of correct classification. It appears, on average, that filters with high radial superposition, are associated with good classification performance, while the effect of circumferential superposition is not significant. We think that this result is worthy of note, being suggestive of alternative filter design approaches from that commonly adopted in literature approaches, where minimization of redundancy among the filters of the bank is considered a good practice.

6. Conclusions

The design of a proper Gabor filter bank is usually a crucial step in texture classification. Despite Gabor filtering has emerged as one of the leading techniques for texture classification, a unifying approach to its adoption has not emerged yet. In this work we have evaluated the effect of Gabor filter parameters on texture classification. In order to perform our study in a systematic way, we have adopted a statistical strategy: the design of experiments. Analysis of the results obtained by applying different Gabor filter banks over different groups of textures led us to some interesting findings. One remarkable outcome is that an increase in the number of frequencies and orientations has, on average, little effect on texture classification. Conversely, the smoothing parameters η and γ are significant factors, and therefore they have to be chosen carefully when designing a Gabor filter bank. Another salient conclusion can be drawn by studying the correlation between the correct classification rate and the overlap (both radial as well as circumferential) of the filters. We found that certain degree of superposition between filters improves classification accuracy. Moreover, comparison between options 1 and 2 gives rise to an alternative method of Gabor filter design. In view of the results, γ should be chosen carefully, and the highest central frequency of the filter bank should be calculated according to Eq. (10), in contrast to the traditional approach, where the highest frequency is set at fixed values as a driving parameter.

Such results appear in agreement with those obtained in Ref. [5], where the authors stated that increasing the number of scales and orientations does not necessarily improve performance. The results reported here are also in accordance with the trend obtained by Li and Shawe-Taylor [14], where the percentage of correct classification shows little variations with n_F and n_O ranging from 4 to 6.

7. Future work

The identification of the significant parameters and of their related trends suggests a possible direction for the optimization of Gabor filters for texture classification, now reducing the independent variables to those parameters that emerged as significant in the above summarized analysis.

Acknowledgments

This work was supported by the *Consiglio Nazionale delle Ricerche* (Italy), under the Grant No. 1402 of the short term mobility program 2005, and by the *Xunta de Galicia* (Spain), under the Grant No. PGIDIT04REM303003PR.

Appendix A. Definition of radial overlap

Radial overlap is computed considering the radial superposition between the half-peak iso-curves of the filter at the highest frequency and orientation 0° ($F1$ in Fig. A.1) and of the filter at the second highest frequency ($F2$ in Fig. A.1) and orientation 0°.

Given $P1$ the lowest radial value of the iso-curve of the filter at the highest frequency, and $P2$ the highest radial value of the iso-curve of the filter at the second highest frequency, the radial overlap is

$$R_o = P_2 - P_1. \tag{A.1}$$

From this definition it follows that:

- $R_o = 0$ when the half-peak magnitude iso-curves are tangent along the radial direction;
- $R_o < 0$ when there is a gap between the half-peak magnitude iso-curves along the radial direction; and
- $R_o > 0$ when there is overlap between the half-peak magnitude iso-curves the radial direction.

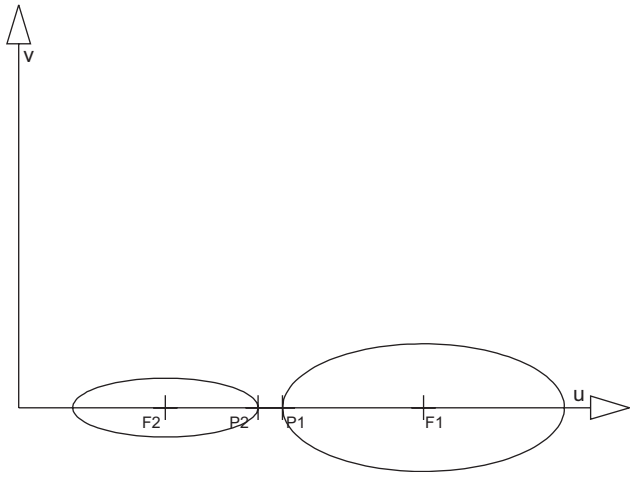

Fig. A.1. Radial overlap.

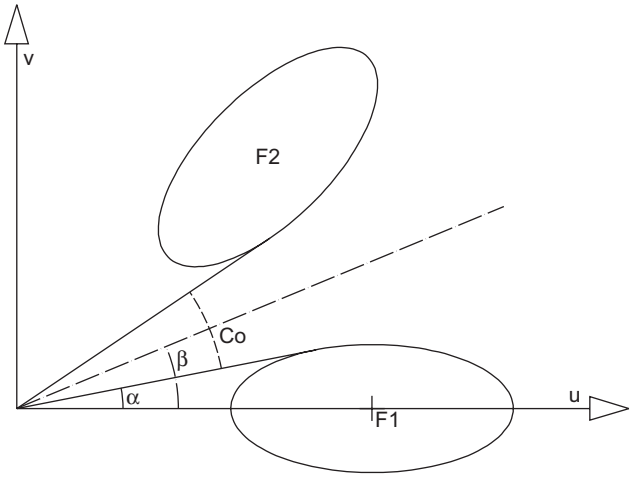

Fig. B.1. Circumferential overlap.

Appendix B. Definition of circumferential overlap

Circumferential overlap is computed considering the circumferential superposition between the half-peak iso-curves of the filter at the highest frequency and orientation 0° ($F1$ in Fig. B.1) and of the filter at the highest frequency ($F2$ in Fig. B.1) and orientation π/n_O.

Let α be the angle between the tangent to the half-peak iso-curves of the filter at the highest frequency and the u axis, and $\beta = \pi/n_O$. The circumferential overlap is defined as follows:

$$C_o = 2\left(\alpha - \frac{\beta}{2}\right). \tag{B.1}$$

From Eq. (B.1) it follows that:

- $C_o = 0$ when the half-peak magnitude iso-curves are tangent along the circumferential direction;
- $C_o < 0$ when there is a gap between the half-peak magnitude iso-curves along the circumferential direction; and
- $C_o > 0$ when there is overlap between the half-peak magnitude iso-curves along the circumferential direction.

Appendix C. F_M as a function of γ

Setting $\Psi(u, v) = \frac{1}{2}$ in Eq. (3), it gives the equation of the half-peak magnitude iso-curve:

$$\frac{\pi^2\gamma^2}{F^2\log(2)}(u' - F)^2 + \frac{\pi^2\eta^2}{F^2\log(2)}v'^2 = 1. \tag{C.1}$$

This is an ellipse of semiaxes:

$$a = \frac{F\sqrt{\log(2)}}{\pi\gamma}; \quad b = \frac{F\sqrt{\log(2)}}{\pi\eta}. \tag{C.2}$$

The maximum frequency value reached by the half-peak magnitude iso-curve of the filter at the highest frequency (F_M) is

then given by

$$F_{max} = F_M \left(1 + \frac{\sqrt{\log(2)}}{\pi\gamma}\right), \tag{C.3}$$

setting now $F_{max} = \frac{1}{2}$, it gives Eq. (10).

References

[1] J.G. Daugman, Uncertainty relation for resolution in space, spatial frequency, and orientation optimized by two-dimensional visual cortical filters, J. Opt. Soc. Am. A 2 (7) (1985) 1160–1169.

[2] D.H. Hubel, T.N. Wiesel, Receptive fields and functional architecture in two nonstriate visual areas 18 and 19 of the cat, J. Neurophysiol. 28 (1965) 229–289.

[3] D.A. Pollen, S.F. Ronner, Visual cortical neurons as localized spatial frequency filters, IEEE Trans. Systems Man Cybern. 13 (5) (1983) 907–916.

[4] T.S. Lee, Image representation using 2D Gabor wavelets, IEEE Trans. Pattern Anal. Mach. Intell. 18 (10) (1996) 959–971.

[5] L. Chen, G. Lu, D. Zhang, Effects of different Gabor filter parameters on image retrieval by texture, in: Proceedings of the 10th IEEE International Multimedia Modelling Conference, Brisbane, Australia, 2004, pp. 273–278.

[6] J.K. Kamarainen, Feature extraction using Gabor filters. Ph.D. Dissertation, Lappeenranta University of Technology, 2003.

[7] P. Vautrot, N. Bonnet, M. Herbin, Comparative study of different spatial/spatial-frequency methods (Gabor filters, wavelets, wavelets packets) for texture segmentation/classification, in: Proceedings of the IEEE International Conference on Image Processing, Lausanne, Switzerland, 1996, pp. 145–148.

[8] M.R. Turner, Texture discrimination by Gabor functions, Biol. Cybern. 55 (1986) 71–82.

[9] A.K. Jain, F. Farrokhnia, Unsupervised texture segmentation using Gabor filters, Pattern Recognition 24 (12) (1991) 1167–1186.

[10] B.S. Manjunath, W.Y. Ma, Texture features for browsing and retrieval of image data, IEEE Trans. Pattern Anal. Mach. Intell. 18 (8) (1996) 837–841.

[11] A.K. Jain, N.R. Ratha, S. Lakhsmanan, Object detection using Gabor filters, Pattern Recognition 30 (2) (1997) 295–309.

[12] P. Kruizinga, N. Petkov, Nonlinear operator for oriented texture, IEEE Trans. Image Process. 8 (10) (1999) 1395–1407.

[13] Y. Rubner, Perceptual metrics for image database navigation, Technical Report CS-TR-99-1621, Stanford University, 1999.

[14] S. Li, J. Shawe-Taylor, Comparison and fusion of multiresolution features for texture classification, Pattern Recognition Lett. 26 (2004) 633–638.

[15] D.A. Clausi, H. Deng, Design-based texture feature fusion using Gabor filters and co-occurrence probabilities, IEEE Trans. Image Process. 14 (7) (2005) 925–936.

[16] T. Randen, J.H. Husøy, Multichannel filtering for image texture segmentation, Opt. Eng. 33 (8) (1994) 2617–2625.

[17] E.P. Simoncelli, W.T. Freeman, E.H. Adelson, D.J. Heeger, Shiftable multiscale transforms, IEEE Trans. Inf. Theory 38 (2) (1992) 587–607.

[18] T. Ojala, T. Mäenpää, M. Pietikäinen, J. Viertola, J. Kyllönen, S. Huovinen, Outex—new framework for empirical evaluation of texture analysis algorithms, in: Proceedings of the 16th International Conference on Pattern Recognition, Quebec, Canada, 2002. pp. 701–706.

[19] P. Brodatz, Textures: A Photographic Album for Artists and Designers, Dover Publications, New York, 1999.

[20] L. Lepistö, I. Kunttu, J. Autio, A. Visa, Classification method for colored natural textures using Gabor filtering, in: Proceedings of the 12th IEEE International Conference on Image Analysis and Processing, 2003.

[21] C.B.R. Ng, G. Lu, D. Zhang, Performance study of Gabor filters and rotation invariant Gabor filters, in: Proceedings of the 11th IEEE International Multimedia Modelling Conference, Melbourne, Australia, 2005.

[22] T. Randen, J.H. Husøy, Filtering for texture classification: a comparative study, IEEE Trans. Pattern Anal. Mach. Intell. 21 (4) (1999) 291–310.

[23] Y. Rubner, J. Puzicha, C. Tomasi, J.M. Buhmann, Empirical evaluation of dissimilarity measures for color and texture, Comput. Vision Image Understanding 84 (2001) 25–43.

[24] F. Bianconi, A. Fernández, Granite texture classification with Gabor filters, in: Actas del XVIII Congreso Internacional de Ingeniería Gráfica, Sitges, Spain, 2006.

[25] A.M. Molinaro, R. Simon, R.M. Pfeiffer, Prediction error estimation: a comparison of resampling methods, Bioinformatics 21 (15) (2005) 3301–3307.

[26] D.C. Montgomery, Design and Analysis of Experiments, fifth ed., Wiley Interscience, 2000.

[27] V. Van Raad, Design of Gabor wavelets for analysis of texture features in cervical images, in: Proceedings of the 25th Annual International Conference on IEEE EMBS, Cancun, Mexico, 2003, pp. 806–809.

[28] R. Manthalkar, P.K. Biswas, B.N. Chatterji, Rotation invariant texture classification using even symmetric Gabor filters, Pattern Recognition Lett. 24 (12) (1993) 2061–2068.

About the Author—FRANCESCO BIANCONI received a Laurea degree in Mechanical Engineering in 1997 from the University of Perugia (Italy), and a Ph.D. in Computer-aided Design in 2000 from a consortium of Italian universities. He is currently Assistant Professor of Design Tools and Methods in Industrial Engineering at the Faculty of Engineering, University of Perugia, Italy. He has worked as visiting researcher at the MIT (USA) and at the University of Vigo (Spain). His research interests are mainly focused on image processing and CAD/CAE. He is member of ACM and IEEE.

About the Author—ANTONIO FERNÁNDEZ was born in Vigo, Spain, in 1967. He graduated as an Industrial Engineer in 1993 from the University of Vigo, and received the Ph.D. degree in Industrial Engineering (with special distinction) in 1998 from the same institution, where he has developed most of his career. He held a research fellowship in the Department of Applied Physics during the period 1994–1998, and subsequently was an Associate Lecturer with the Department of Engineering Design form 1999 to 2003. Since then he has been a Senior Lecturer, and the Head of the Colorimetry Research Group. He has worked as a visiting researcher at Centre for Research on Optics (Mexico), University of Perugia (Italy), Dublin City University (Ireland) and Computer Vision Centre (Spain). His major research interests include texture analysis and speckle metrology.